



HAL
open science

Dehydrohalogenation of halobenzenes and C(sp³)-X (X = F, OPh) bond activation by a molecular calcium hydride

Andrew S. S. Wilson, Michael S. Hill, Mary F. Mahon, Chiara Dinoi, Laurent Maron

► **To cite this version:**

Andrew S. S. Wilson, Michael S. Hill, Mary F. Mahon, Chiara Dinoi, Laurent Maron. Dehydrohalogenation of halobenzenes and C(sp³)-X (X = F, OPh) bond activation by a molecular calcium hydride. *Tetrahedron*, 2021, 82, 10.1016/j.tet.2021.131931 . hal-03717244

HAL Id: hal-03717244

<https://hal.science/hal-03717244>

Submitted on 22 Mar 2023

HAL is a multi-disciplinary open access archive for the deposit and dissemination of scientific research documents, whether they are published or not. The documents may come from teaching and research institutions in France or abroad, or from public or private research centers.

L'archive ouverte pluridisciplinaire **HAL**, est destinée au dépôt et à la diffusion de documents scientifiques de niveau recherche, publiés ou non, émanant des établissements d'enseignement et de recherche français ou étrangers, des laboratoires publics ou privés.



Distributed under a Creative Commons Attribution - NonCommercial 4.0 International License

Dehydrohalogenation of halobenzenes and C(sp³)-X (X = F, OPh) bond activation by a molecular calcium hydride

Andrew S. S. Wilson,¹ Michael S. Hill,^{1*} Mary F. Mahon,¹ Chiara Dinoi² and Laurent Maron^{2*}

¹ Department of Chemistry, University of Bath, Claverton Down, Bath, BA2 7AY, UK

² Université de Toulouse et CNRS, INSA, UPS, UMR 5215, LPCNO, 135 Avenue de Rangueil, F-31077 Toulouse, France

Email : msh27@bath.ac.uk; laurent.maron@irsamc.ups-tlse.fr

Abstract

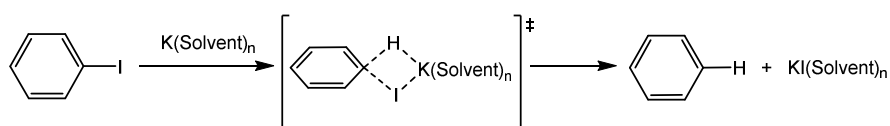
The molecular calcium hydride, [(BDI)CaH]₂ (BDI = HC{(Me)CN-2,6-*i*-Pr₂C₆H₃}₂), effects the slow hydrodehalogenation of C₆H₅X (X = I, Br) to provide benzene and the respective dimeric calcium halides, [(BDI)CaX]₂. Although the analogous hydrogenation of chlorobenzene is observed, this process yields the calcium hydride-chloride as the alkaline earth-containing product. Assessment of the bromide- and chloride-based processes by density functional theory (DFT) calculations, imply that the reactions take place with the retention of the dimeric calcium structures throughout. Both systems invoke an S_NAr-type displacement of the halide, via barriers (ca. 32 – 34 kcal mol⁻¹), which vary only marginally during the transformation of the initial hydride and halide-hydride intermediates. The isolation of the calcium hydride-chloride is ascribed, therefore, to its more rapid crystallisation and depletion from solution. Also reported is the reactivity of [(BDI)CaH]₂ with α,α,α -trifluorotoluene and anisole, which yield the corresponding dicalcium hydride-fluoride and phenoxide derivatives, respectively, rather than the products of directed ortho metalation

Keywords: Calcium · Hydride · halobenzene · dehydrohalogenation

Introduction

From the synthesis of medicinal compounds to agrochemicals, aromatic substitution reactions provide a broadly useful platform for the modification of aromatic ring scaffolds and are of pivotal importance in many organic transformations. Although a majority of such transformations operate by the addition of appropriate electrophiles to electron-rich arene π systems (i.e. electrophilic aromatic substitution),¹ it has long been recognised that alternative nucleophilic substitution (S_NAr) pathways are also accessible, particularly for arene systems bearing electron withdrawing substituents.^{2,3} Although a majority of S_NAr processes require the stepwise formation of a discrete, non-aromatic Meisenheimer intermediate, a number of studies have lent credence to the operation of alternative *concerted* substitution (cS_NAr) pathways.^{4,5} Of particular relevance to the current contribution, are Chiba's report of the hydrodehalogenation of haloarenes with a sodium hydride–iodide composite and Tuttle and Murphy's recent account of the role of potassium hydride in haloarene reduction (Scheme 1).⁶⁻⁸

Foreshadowed by an earlier empirical study by Pierre and co-workers,⁹ this latter study employed a combination of experimental and computational techniques to demonstrate that concerted displacement of halide from haloarenes is initiated by attack of the naked hydride donor at the π^* orbital of the aromatic ring. Although evidence for single electron transfer was observed for reactions performed in benzene, the formation of benzyne intermediates was discounted under all conditions, and a cS_NAr mechanism was deduced to predominate in procedures carried out in THF. In contrast, although documented examples are sparse, related reports of the reactivity of molecular lanthanide or d^0 transition metal hydrides with halobenzenes are typically complicated by the formation of the reactive benzyne intermediate via *ortho*-metalation and cleavage of the C-halogen bond.¹⁰

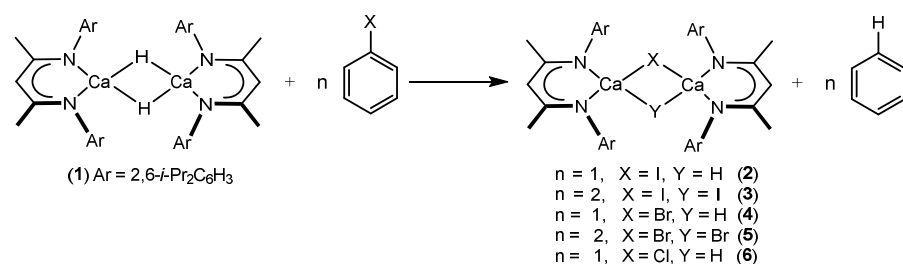


Scheme 1: Concerted nucleophilic aromatic substitution (cS_NAr) by potassium hydride and the hydrodehalogenation of iodobenzene.^{8,4,9}

Our current interest in these processes derives from recent advances arising from the chemistry and reactivity of heavier alkaline earth hydride derivatives.¹¹⁻²⁹ Our particular focus has been provided by the molecular β -diketiminato calcium hydride, [(BDI)CaH]₂ (**1**; BDI = HC{(Me)CN-2,6-*i*-Pr₂C₆H₃}₂), which serves as a potent source of the hydride nucleophile.³⁰⁻³⁸ We have previously reported that the hydride ligands of compound **1** react in a stepwise fashion and through retention of its dimeric structure during their nucleophilic addition to accessible C=C bonds in alkenes and even the high energy π systems of aromatic hydrocarbons.^{38,34} While the former reactions give rise to a range of calcium alkyl derivatives, which are themselves sufficiently reactive to effect the nucleophilic activation of H₂ and benzene,^{31,30,39} the outcome of hydride addition to a range of polyaromatic hydrocarbons displayed an apparent dependence on the energy of the relevant π^* system and could be correlated with the arene reduction potential (E^0).³⁴ Whereas degenerate Ca-H/C-H exchange between benzene ($E^0 = ca. -3.4$ V) and compound **1** was calculated to involve a high energy nucleophilic attack of hydride (ΔH^\ddagger 35.5 kcal mol⁻¹), similar disruption of the aromaticity of tetracene, anthracene or naphthalene induced facile loss of atomic hydrogen and the formation of a radical anion intermediate *en route* to the ultimate arene dianion products of two electron reduction. While the reduction of naphthalene ($E^0 = ca. -3.4$ V), in particular, indicates that compound **1** presents as a highly potent molecular reducing agent, the reaction with benzene may be viewed as broadly analogous to the dehalogenative processes depicted in Scheme 1b. In this study, therefore, we report our initial observations of the reactivity of compound **1** with the monohalobenzenes, C₆H₅X (X = I, Br, Cl, F) and related transformations with α,α,α -trifluorotoluene and anisole.

Results and Discussion

Hydrodehalogenation of halobenzenes. Immediate analysis of a reaction between compound **1** and two equivalents of iodobenzene in C_6D_6 at room temperature provided a 1H NMR spectrum comprising two predominant compounds. The dicalcium hydride-iodide (**2**) was tentatively identified by the emergence of a γ -methine BDI signal at 4.76 ppm, while the formation of the dimeric calcium iodide [**3**, δ 4.84 (γ - C_{BDI}) ppm] was subsequently confirmed by its independent isolation in analytically pure form (*vide infra*). The signals arising from compounds **2** and **3**, along with a minor quantity of $[(BDI)_2Ca]$ (δ 4.94 (γ -C) ppm),⁴⁰ were observed to integrate in an approximate ratio of 2:3:1, while the production of additional C_6H_6 was evidenced by a clear increase in intensity of the signal associated with the residual protio resonance of C_6D_6 (Scheme 2). An analogous reaction of two equivalents of bromobenzene and **1** similarly afforded a 1H NMR spectrum containing a mixture of unreacted **1**, an intermediate species cautiously assigned as the dicalcium hydride-bromide [**4**, δ 4.76 (γ - C_{BDI}) ppm] and the dimeric calcium bromide, $[(BDI)CaBr]_2$ [**5**, δ 4.82 (γ - C_{BDI}) ppm] (Scheme 2). Although the 1H NMR spectrum of this reaction mixture was effectively unchanged after one day at room temperature, a further reaction of **1** with a *ca.* 100-fold excess of bromobenzene afforded a 1H NMR spectrum that consisted predominantly of compound **5** after three days at room temperature.



Scheme 2: Reaction of **1** with halobenzenes.

In contrast to the facility of the reactions with its heavier halide congeners, initial analysis of a reaction performed with two equivalents of chlorobenzene and **1** provided a 1H NMR spectrum arising entirely from the unreacted starting materials. After one week at room temperature, however, the consumption of *ca.* 50% of the initial quantity of **1** was accompanied by the emergence of the dicalcium hydride-chloride (**6**), which could be identified in the 1H NMR spectrum by the appearance of a new γ - CH_{BDI} resonance at δ 4.85 ppm, and which integrated in an approximate 2:1 ratio with an accompanying hydride signal at δ 3.95 ppm. A subsequent reaction between **1** and an excess of chlorobenzene afforded almost exclusive formation of compound **6** after one day at room temperature.

In a similar manner to the reaction with C_6H_5Cl , addition of two equivalents of fluorobenzene to a C_6D_6 solution of **1** provided a 1H NMR spectrum solely indicative of the unreacted starting materials at the first point of analysis. Storage at room temperature for four days, however, afforded an intractable mixture of unidentified compounds. Although residual unreacted fluorobenzene could

be identified in the $^{19}\text{F}\{^1\text{H}\}$ NMR spectrum ($\delta -112.9$ ppm), this resonance was observed alongside a series of similar but unassignable fluorine resonances at $\delta -75.5$, -74.3 , -72.8 , -72.2 , -70.3 and -44.7 ppm.

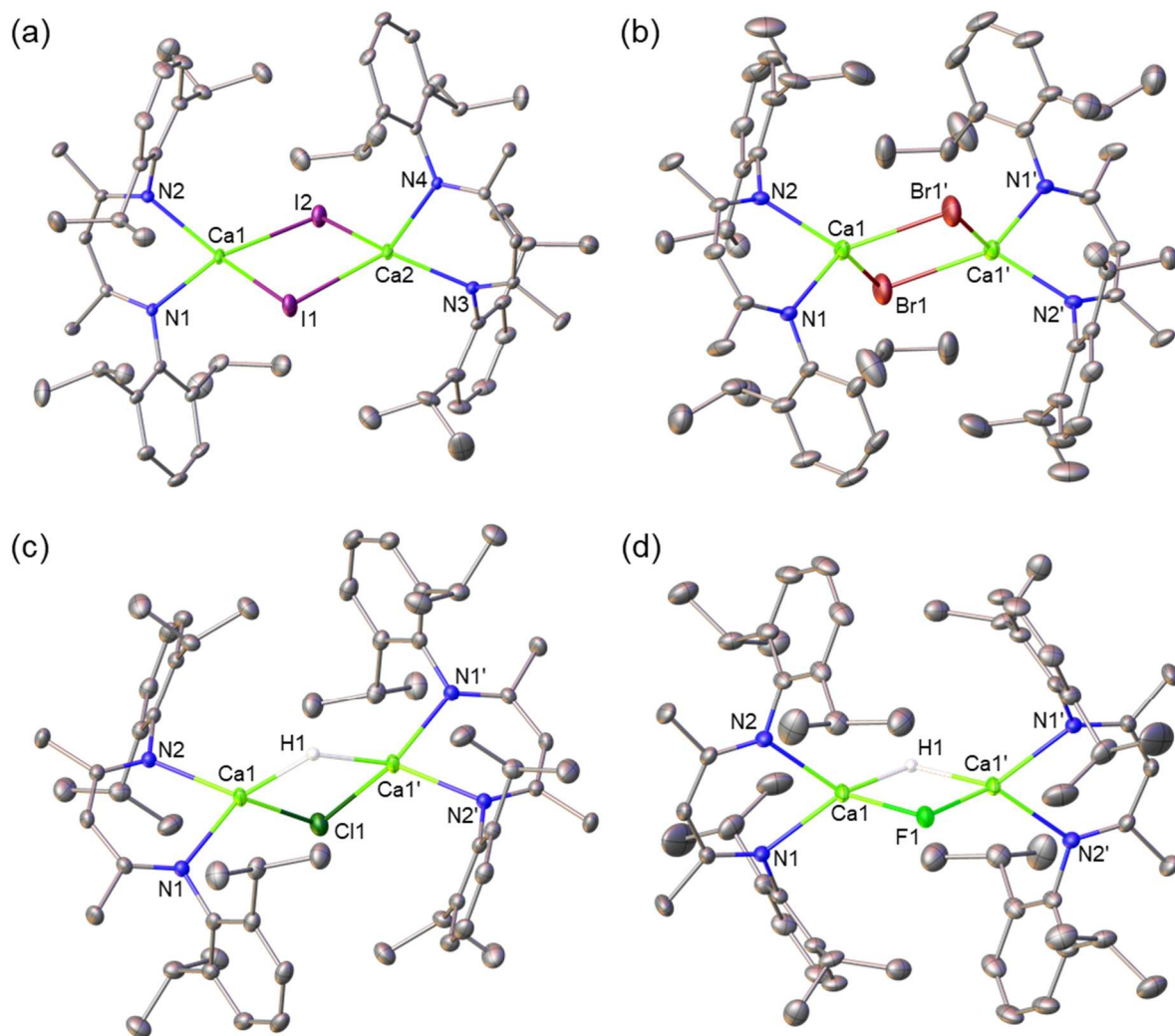


Figure 1: ORTEP s of compound (a) compound **3**, (b) compound **5**, (c) compound **6** and (d) compound **7** with thermal ellipsoids at 30%. Hydrogen atoms, except H1 of compounds **6** and **7**, have been omitted for clarity. Symmetry operations to generate primed atoms: (**5**) $1-x, 1-y, -z$; (**6, 7**) $1-x, -y, -z$.

Table 1: Selected bond (Å) and angles (°) of **3**, **5**, **6**, **7** and **8**.

	3 (X = I)	5 (X = Br) ^a	6 (X = Cl) ^b	7 (X = F) ^b	8 (X = OPh) ^c
Ca1-N1	2.3009(16)	2.2969(17)	2.3051(13)	2.3114(11)	2.3546(11)
Ca1-N2	2.2768(15)	2.3019(18)	2.3049(13)	2.3273(12)	2.3355(10)
Ca2-N3	2.2895(15)	-	-	-	-
Ca2-N4	2.2848(16)	-	-	-	-
Ca1-X1	3.0798(4)	2.7977(7)	2.6388(11)	2.173(3)	2.3012(10)
Ca1'-X1	-	2.8309(6)	2.6770(11)	2.178(3)	2.2425(9)
Ca1-X2	3.0595(4)	-	-	-	-
Ca2-X1	3.0336(4)	-	-	-	-
Ca2-X2	3.0919(4)	-	-	-	-
N1-Ca1-N2	82.53(5)	80.52(6)	81.43(5)	79.26(4)	79.63(4)
N3-Ca2-N4	82.90(5)	-	-	-	-
Ca1-X1-Ca2/Ca'	86.182(11)	89.960(17)	83.82(3)	102.71(16)	102.03(4)
Ca1-X2-Ca2	85.523(11)	-	-	-	-

Symmetry operations to generate primed atoms: ^a 1-x, 1-y, -z; ^b 1-x, -y, -z; ^c -x, -y, 1-z.

The veracity of the deductions arising from the *in situ* analysis of these reactions was supported by the characterisation of pure samples of compounds **3**, **5** and **6**, which were isolated as single crystals suitable for X-ray diffraction analysis either from the reaction mixture (**3**) or from toluene/hexane solutions (**5**, **6**). The results of the solid-state analyses are presented in Figures 1a – 1c and selected bond length and angle data are provided in Table 1. While all three compounds are dinuclear with μ_2 -bridging halide or hydride ligands, the iodide derivative (**3**) presents two independent calcium environments whereas both compounds **5** and **6** are centrosymmetric. Compound **3** comprises two distorted tetrahedral calcium centres with Ca-N [2.2768(15) - 2.3009(16) Å], Ca-I [3.0336(4) - 3.0919(4) Å] distances and N-Ca-N angles [82.53(5) and 82.90(5)°] which are significantly shorter and more acute than the respective measurements [Ca-N 2.347(2), 2.367(2); Ca-I 3.1224(8), 3.090(1) Å; N-Ca-N 81.34(8)°] of the previously reported, but ether adducted, calcium iodide, [(BDI)CaI(Et₂O)]₂.⁴¹ The gross structures of compounds **5** and **6** are similar to that of **3** with closely comparable Ca-N [2.28 - 2.31 Å] distances and N-Ca-N angles [81.4 - 82.9°]. As expected, however, the Ca-X bonds elongate from approximately 2.6 Å (**3**) to 2.8 Å (**5**) to 3.0 Å (**6**) with the increasing ionic radius of the bridging halide atoms.⁴² As a consequence of the crystallographic symmetry in **6**, the bridging ligands were disordered in the gross structure. The H1 assignment, therefore, was made to a residual electron density peak in the penultimate difference Fourier map, and the final least-squares were conducted with the restraint of both Ca-H distances being similar. With this proviso in place, the Ca-H [2.05(4) and 2.07(3) Å] and Ca-Cl [2.6388(11) and 2.6770(11) Å] distances of **6** are

within the ranges established for the independent Ca-H [2.17(2) and 2.225(16) Å] distances of **1** and the Ca-Cl [2.676(1) and 2.685(1) Å] bond lengths of [(BDI)CaCl(THF)]₂,⁴³ despite the coordinated THF molecule in this latter compound.

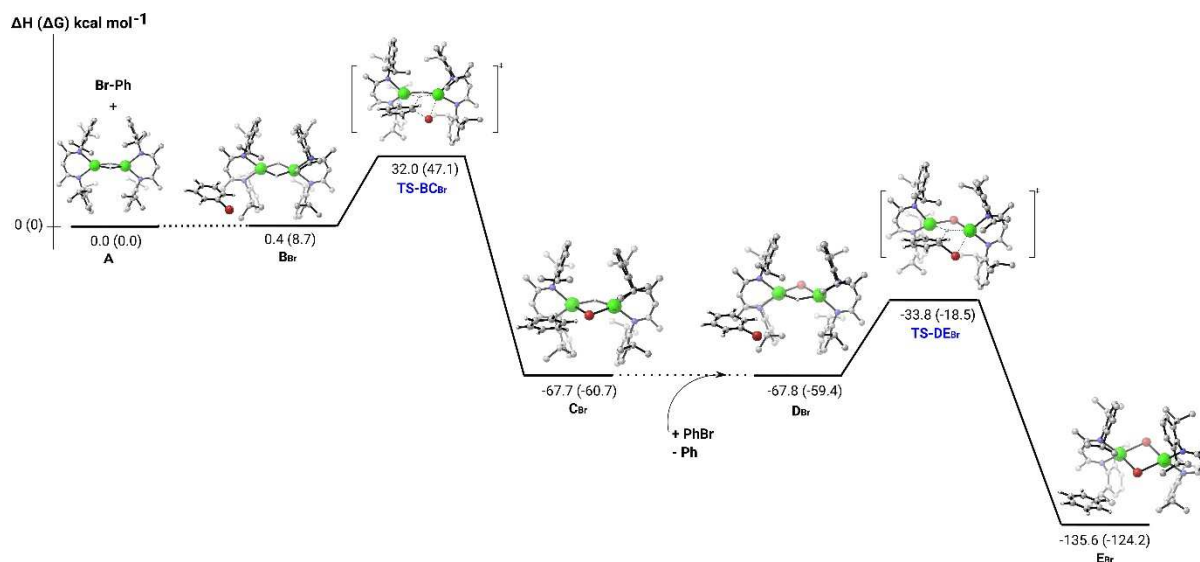


Figure 2: Computed enthalpy (Gibbs free energy in parenthesis) profile for the reaction of bromobenzene with complex **1** at room temperature.

Calculations were carried out at the DFT level (B3PW91) in order to get some insights onto the formation of complexes **4**, **5** and **6** from the reaction of either bromo- or chloro-benzene with **1**. For clarity, only the reaction of **1** with bromobenzene, that is the formation of **4** and **5**, will be discussed in detail. The formation of **6** is presented in the ESI (Figure S24).

The lowest energy profile is presented in Figure 2 but other possible reactions were computed and were found to be higher in energy (see Figure S25). As was the case in previous observations of compound **1**,^{30,31} the reaction is found to occur at the dicalcium complex since the dimer disruption energy is more than 40.4 kcal mol⁻¹. After the formation of a loosely bonded bromobenzene adduct (**B**_{Br}, +0.4 kcal mol⁻¹), a S_NAr-type transition state (**TS-BC**_{Br}) has been located. Consistent with the relatively slow reaction observed, the associated barrier is 32.0 kcal mol⁻¹. Following the intrinsic reaction coordinate yields the formation of the very stable benzene solvated complex **4** (**C**_{Br}), whose formation is exothermic by 67.7 kcal mol⁻¹. The latter reaction energy indicates that the experimental time scale for the completion of the reaction is a direct consequence of the height of this barrier. Subsequent benzene to bromobenzene exchange is athermic but allows complex **4** to undergo a further S_NAr-type reaction via a similar barrier of 34.0 kcal mol⁻¹. From this perspective, therefore, the remaining hydride in complex **4** appears to be almost as reactive as that invoked in its own generation from complex **1**. Although the formation of the solvated version of complex **5** (**E**_{Br}) is again highly exothermic (-135.6 kcal mol⁻¹ with respect to the entrance channel, -67.9 kcal mol⁻¹,

from C_{Br}), the barriers associated with the production of both **4** and **5** are effectively identical, irreversible and consistent with the experimental observations of relatively slow reactions. It is noteworthy that the inclusion of dispersion effect led to a similar profile as that reported in Figure 2. The associated barriers, however, are too low and inconsistent with a reaction needing three days at room temperature for completion (see Figure S26). We ascribe this observation as an artefact resulting from an overestimation of the attractive interactions in the bimetallic species and a resultant lowering of the barriers.

The formation of complex **6** was computed to follow a similar pathway as that shown in Figure 2 (Figure S24) with similar barrier. The lack of formation of the chloride equivalent of complex **5** is, thus, attributed to the rapid crystallisation of complex **6** (C_{Cl} in Figure S24), which prevents further reaction.

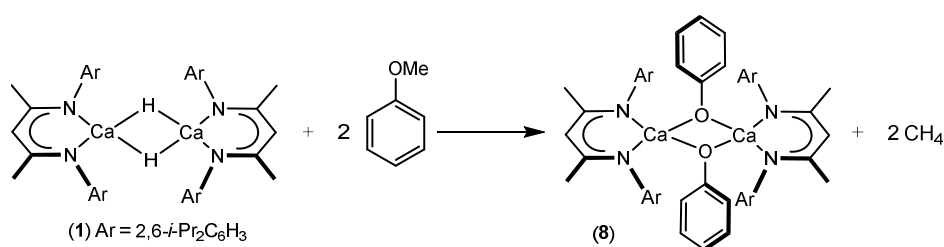
Reactivity of compound 1 and α,α,α -trifluorotoluene and anisole. The contrasting reactivity of **1** with fluorobenzene was tentatively ascribed as a consequence of initial *ortho*-metalation and subsequent benzyne formation. Similar processes have previously been deduced for reactions between the range of halobenzenes utilised herein and $[Cp^*_2YH]_2$.¹⁰ This reactivity is also reminiscent of directed *ortho*-metalation (DoM) chemistry, in which aromatic substituents such as an amide or methoxy group are employed to direct the site of metalation by organolithium reagents, and which continues to be a widely employed strategy to effect the regioselective functionalisation of substituted aromatic and heteroaromatic compounds.⁴⁴⁻⁴⁷ The trifluoromethyl substituent of α,α,α -trifluorotoluene is known to induce pronounced increases in the acidity of the aryl-hydrogen bonds. This is particularly acute at the *ortho* positions, which are readily deprotonated by s-block organometallics such that, for example, the regioselective *ortho*-metalation of α,α,α -trifluorotoluene has been achieved with *n*-butyllithium,^{48,49} *n*-butylsodium,⁵⁰ the alkali metal zincate $[NaZn(TMP)t-Bu_2]$ (TMP = 2,2,6,6-tetramethylpiperidine),⁵¹ the aluminate $[LiAl(TMP)t-Bu_3]$ ⁵² and the magnesiate $[(PMDETA)_2K_2Mg(CH_2SiMe_3)]$ (PMDETA = *N,N,N',N'',N'''*-pentamethyldiethylenetriamine).⁵³ Notably, the sodium magnesiate inverse crown complex $[Na_4Mg_2(TMP)_6(n-Bu)_2]$ selectively *ortho,meta*-dimetalates α,α,α -trifluorotoluene via a templating motif.⁵⁴

In a similar manner, the methoxy substituent of anisole effects predominant *ortho*-metalation via inductive and complex-induced proximity effects.⁵⁵ DoM of anisole was initially observed with *n*-BuLi and PhLi during the seminal studies of Gilman⁵⁶ and Wittig.⁵⁷ Directed *ortho*-lithiation has since been investigated with NMR spectroscopy,⁵⁸ computational calculations,^{58,59} isotopically labelled experiments⁶⁰ and X-ray crystallography.⁶¹ Similarly, *ortho* deprotonation with alkali metal zincate, $[(THF)LiZn(TMP)(t-Bu)_2]$,⁶² aluminate, $[(THF)LiAl(TMP)_2(i-Bu)_2]$,⁶³ and magnesiate, $[(PMDETA)KMg(TMP)_2(CH_2SiMe_3)]$,⁶⁴ complexes has been readily achieved.

Based on these significant precedents, therefore, it was postulated that the basicity of compound **1** may enable the deprotonation of α,α,α -trifluorotoluene and anisole in a similar fashion.

Immediate assessment of a reaction between two equivalents of α,α,α -trifluorotoluene and **1** in C_6D_6 afforded a 1H NMR spectrum containing only unreacted starting materials. Continued monitoring over 7 days, however, demonstrated the slow formation of the calcium hydride-fluoride $[(BDI)Ca]_2(\mu-F)(\mu-H)$ (**7**), which was identified by the appearance of diagnostic doublet resonances at δ 3.84 ppm and δ -42.0 ppm in both the 1H and ^{19}F NMR spectra ($^2J_{HF} = 37.3$ Hz). Although the mechanism of fluoride abstraction was not investigated in detail, the absence of a ^{19}F resonance attributable to $C_6H_5CHF_2$ [$\delta(^{19}F)$ -111 ppm]⁶⁵ and the appearance of unidentified singlet resonances in the ^{19}F NMR spectrum at δ -63.0, -72.8 and -83.8 ppm indicates that the reaction is unlikely to be predicated solely on a direct metathetical Ca-H/F-C exchange process.

Despite the apparent complexity of the reaction, and in a similar manner to the reactions with halobenzenes described above, treatment of **1** with a *ca.* 100-fold excess of α,α,α -trifluorotoluene afforded a solution that contained predominantly compound **7** [δ 4.83 (Ca-H), 3.84 (γ -C_{BDI}) ppm] after only one day at room temperature. Monitoring of this solution by 1H and ^{19}F NMR spectroscopy confirmed that compound **7** persisted in solution and provided no detectable evidence for redistribution to either compound **1** or $[(BDI)CaF]_2$. Crystallisation of the reaction mixture from toluene afforded single crystals of **7** suitable for X-ray diffraction analysis (Figure 1d and Table 1). Although the bridging fluoride and hydride ligands are again disordered, the centrosymmetric Ca- μ_2 -F-Ca' bridged structure of compound **7** is comparable to those of the previously reported β -diketiminato calcium fluorides, $[(BDI)CaF(THF)]_2$ and $[HC\{(F_3C)CN(2,6-i-Pr_2C_6H_3)\}_2CaF(THF)]_2$.^{66,67} Despite the additional molecules of THF within the calcium coordination spheres of both of these previously reported compounds, the μ_2 -F-Ca bond lengths of **7** lie within the established range [**7**: 2.173(3), 2.178(3); $[(BDI)CaF(THF)]_2$: 2.170(2), 2.189(2); $[HC\{(F_3C)CN(2,6-i-Pr_2C_6H_3)\}_2CaF(THF)]$ 2.168(2), 2.186(2) Å].



Scheme 3: Synthesis of compound **8**.

Although no reaction was observed by 1H NMR spectroscopy between two equivalents of anisole and **1** in C_6D_6 over a duration of 16 hours, heating the solution at 60 °C for a similar period induced the formation of a single new β -diketiminato derivative, compound **8**, which was most clearly characterised by a new γ -C_{BDI} signal at δ 4.91 ppm. The formation of compound **8** was accompanied by the appearance of a further singlet resonance at δ 0.16 ppm, which was readily attributed to methane.⁶⁸ The origin of these observations was resolved by removal of deuterobenzene and

crystallisation of the solid residue from toluene. The resultant single crystal X-ray analysis confirmed the identify of **8** as the calcium phenoxide derivative, [(BDI)CaOPh]₂ (Figure 3, Table 1), and the overall stoichiometry of the reaction shown in Scheme 3. The calcium centres of the centrosymmetric structure of **8** are coordinated by typical calcium-nitrogen interactions from the β -diketiminato ligand [2.3546(11) and 2.3355(10) Å] and bridging phenoxide ligands, the Ca-O bond lengths of which [2.3012(10) and 2.2425(9) Å] lie within the range of previously reported bridging aryloxide Ca- μ_2 -O-Ca interactions (2.25 - 2.37 Å).⁶⁹⁻⁷²

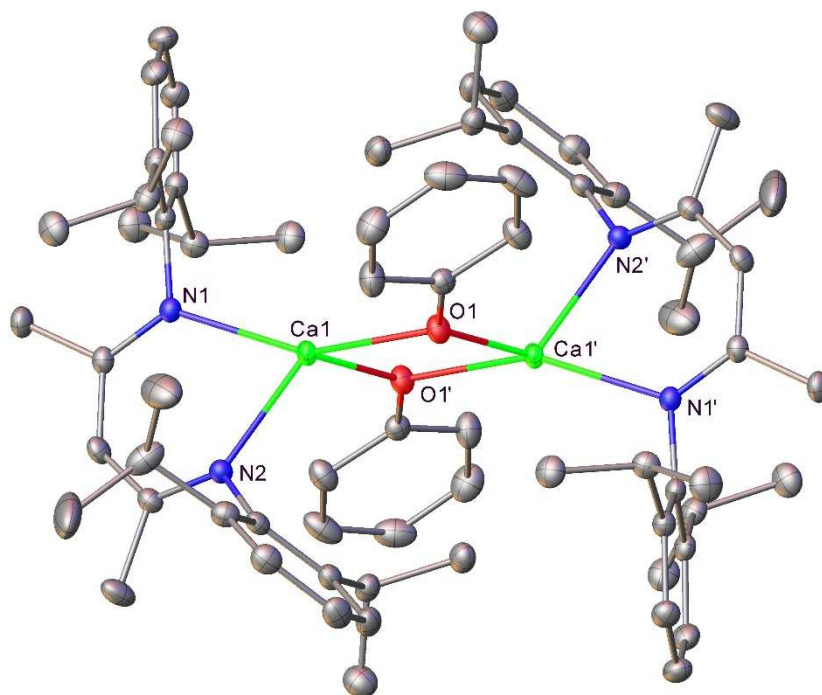


Figure 3: ORTEP representation of compound **8** with thermal ellipsoids at 30%. Hydrogen atoms have been omitted for clarity. Atoms with primed labels related to those in the asymmetric unit by the $-x, -y, 1-z$ symmetry operation.

Rather than the anticipated *ortho*-metalation, the generation of **8** and methane (Scheme 3) requires an apparent σ -bond metathesis of the Ca-H bond of **1** with the O-CH₃ bond of anisole. Although the rupture of the C(*sp*³)-O (*ca.* 273 kJ mol⁻¹)⁷³ bond rather than the C(*sp*²)-O (*ca.* 419 kJ mol⁻¹)⁷⁴ bond may be rationalised by the thermochemical preference for the formation of the resultant Ca-O bond (348 kJ mol⁻¹), this process occurs with notable kinetic facility and selectivity. Whilst ether cleavage is well-documented with a plethora of alkali metals and organoalkali compounds,⁷⁵ such a well-defined cleavage of the aliphatic C-O bond of anisole with a molecular metal hydride appears to be unprecedented. The addition of DME to [(BDI)CaH(Et₂O)]₂ has, however, been shown to effect diethyl ether cleavage to provide the calcium ethoxide [(BDI)CaOEt]₂.⁷⁶ Similarly, the cerium hydride [Cp'₂CeH] (Cp' = 1,2,4-tri-*tert*-butylcyclopentadienyl) promotes C-O cleavage of a range of

dialkylethers, [RCH₂CH₂OR'] (R = H, Me, Et; R' = CH₂CHR) to the corresponding cerium alkoxides [Cp₂'OR'],⁷⁷

In summary, the β -diketiminato calcium hydride (**1**) effects the dehydrohalogenation of iodo- bromo- and chlorobenzene under mild conditions. Furthermore, compound **1** is able to activate strong bonds of α,α,α -trifluorotoluene (C-F; ~ 500 kJmol⁻¹) and anisole (C-O; 273 kJmol⁻¹). Although the outcome of both these latter processes is striking, their viability may be attributed to the resultant thermochemical strength of the resultant Ca-F (557 kJ mol⁻¹) and Ca-O (348 kJ mol⁻¹) bonds.⁷⁴

Experimental Section

All manipulations were carried out using standard Schlenk line and glovebox techniques under an inert atmosphere of argon. NMR experiments were conducted in J Young tap NMR tubes prepared and sealed in a Glovebox. NMR spectra were collected on an Agilent ProPulse spectrometer operating at 500 MHz (¹H), 126 MHz (¹³C), 470 MHz (¹⁹F). The spectra were referenced relative to residual protio solvent resonances or an internal standard. Solvents (toluene, hexane) were dried by passage through a commercially available (MBraun) solvent purification system, under nitrogen and stored in ampoules over 4Å molecular sieves. C₆D₆ was purchased from Sigma-Aldrich Corp., dried over a potassium mirror before vacuum distilling under argon and storing over molecular sieves. Calcium iodide (99.95%) and organic reagents were purchased from Sigma-Aldrich Corp. and either distilled or recrystallised prior to use. [(BDI)CaH]₂ (**1**) was synthesised by a literature procedure.³⁰

Synthesis of [(BDI)CaI]₂ (**3**)

Iodobenzene (7.27 μ L, 0.065 mmol) was added to an unstirred toluene (*ca.* 0.5 ml) solution of **1** (30 mg, 0.033 mmol). After 16 hrs at room temperature hexane (*ca.* 0.5 ml) was added to the resultant pale-yellow solution which was stored at -35 °C to afford colourless crystals of **3** (18 mg, 45%). Single crystals suitable for X-ray diffraction analysis were obtained directly from the analogous NMR scale reaction of iodobenzene with **1** in C₆D₆. ¹H NMR (500 MHz, benzene-d₆) δ 7.18 - 7.14 (m, 6H, Ar-H), 4.84 (s, 1H, NC(CH₃)CH), 3.10 (hept, ³J_{HH} = 6.8 Hz, 4H, CH(CH₃)₂), 1.65 (s, 6H, NC(CH₃)CH), 1.25 (d, ³J_{HH} = 6.8 Hz, 12H, CH(CH₃)₂), 1.13 (d, ³J_{HH} = 6.8 Hz, 12H, CH(CH₃)₂) ppm. ¹³C{¹H} NMR (126 MHz, benzene-d₆) δ 166.5 (NC(CH₃)CH), 142.1 (*C*_{ortho}), 125.5 (*C*_{para}), 124.5 (*C*_{meta}), 95.2 (NC(CH₃)CH), 29.0 (CH(CH₃)₂), 25.9, 24.6 (CH(CH₃)₂), 24.2 (NC(CH₃)CH) ppm. Elemental analysis for C₅₈H₈₂Ca₂I₂N₄: C, 59.58; H, 7.07; N, 4.79%. Found: C, 59.75; H, 7.18; N, 4.76%.

Synthesis of [(BDI)CaBr]₂ (**5**)

Bromobenzene (500 μ L) and C₆D₆ (50 μ L) were added to **1** (30 mg 0.033 mmol) and stored at room temperature for three days affording a pale-yellow solution. The resulting solution was evaporated to

dryness, redissolved in toluene (*ca.* 0.5 ml), layered with hexane (*ca.* 0.5 ml) and cooled to $-35\text{ }^{\circ}\text{C}$ to yield **5** as colourless single crystals (11 mg, 30%). ^1H NMR (500 MHz, benzene- d_6) δ 7.17 - 7.11 (m, 6H, Ar-*H*), 4.84 (s, 1H, NC(CH₃)CH), 3.06 (hept, $^3J_{\text{HH}} = 6.7\text{ Hz}$, 4H, CH(CH₃)₂), 1.66 (s, 6H, NC(CH₃)CH), 1.18 (d, $^3J_{\text{HH}} = 6.7\text{ Hz}$, 12H, CH(CH₃)₂), 1.11 (d, $^3J_{\text{HH}} = 6.7\text{ Hz}$, 12H, CH(CH₃)₂) ppm. $^{13}\text{C}\{^1\text{H}\}$ NMR (126 MHz, benzene- d_6) δ 166.2 (NC(CH₃)CH), 143.2 (*C*_{ipso}), 142.2 (*C*_{ortho}), 125.5 (*C*_{para}), 124.5 (*C*_{meta}), 95.4 (NC(CH₃)CH), 28.9 (CH(CH₃)₂), 25.2, 24.6 (CH(CH₃)₂), 23.9 (NC(CH₃)CH) ppm. Elemental analysis for C₅₈H₈₂Ca₂Br₂N₄: C, 64.79; H, 7.69; N, 5.21%. Found: C, 64.51; H, 7.57; N, 5.18%.

Synthesis of [(BDI)Ca]₂(μ -Cl)(μ -H) (**6**)

Chlorobenzene (500 μL) and C₆D₆ (50 μL) was added to **1** (30 mg 0.033 mmol) and stored at room temperature overnight (*ca.* 16 hrs) affording a pale-yellow solution. The resulting solution was evaporated to dryness, redissolved in toluene (*ca.* 0.5 ml), layered with hexane (*ca.* 0.5 ml) and cooled to $-35\text{ }^{\circ}\text{C}$ to yield **6** as colourless single crystals (8 mg, 25%). ^1H NMR (500 MHz, benzene- d_6) δ 7.13 - 7.06 (m, 12H, Ar-*H*), 4.84 (s, 2H, NC(CH₃)CH), 3.95 (s, 1H, CaH), 3.08 - 3.00 (m, 8H, CH(CH₃)₂), 1.66 - 1.65 (m, 12H, NC(CH₃)CH), 1.15 - 1.05 (m, 48H, CH(CH₃)₂) ppm. $^{13}\text{C}\{^1\text{H}\}$ NMR (126 MHz, benzene- d_6) δ 166.0, 165.7 (NC(CH₃)CH), 143.0, 143.0 (*C*_{ipso}), 142.2, 142.1 (*C*_{ortho}), 125.5, 125.3 (*C*_{para}), 124.5, 124.5 (*C*_{meta}), 94.1 (NC(CH₃)CH), 28.8, 28.6 (CH(CH₃)₂), 25.2, 24.9, 24.7, 24.4 (CH(CH₃)₂), 23.7, 23.7 (NC(CH₃)CH) ppm. Elemental analysis for C₅₈H₈₃Ca₂ClN₄: C, 73.18; H, 8.79; N, 5.89%. Found: C, 73.12; H, 8.92; N, 5.85%.

Synthesis of [(BDI)Ca]₂(μ -F)(μ -H) (**7**)

α,α,α -trifluorotoluene (500 μL) and C₆D₆ (50 μL) was added to **1** (60 mg 0.065 mmol) and stored at room temperature overnight (*ca.* 16 hrs) affording an orange solution. The resulting solution was evaporated to dryness, redissolved in toluene (*ca.* 0.5 ml), layered with hexane (*ca.* 0.5 ml) and cooled to $-35\text{ }^{\circ}\text{C}$ to yield **7** as colourless single crystals (13 mg, 11%). ^1H NMR (500 MHz, benzene- d_6) δ 7.10 - 7.03 (m, 12H, Ar-*H*), 4.83 (s, 2H, NC(CH₃)CH), 3.83 (d, $^3J_{\text{HF}} = 37.3\text{ Hz}$, 1H, CaH), 3.11 - 3.03 (m, 8H, CH(CH₃)₂), 1.66 - 1.65 (m, 12H, NC(CH₃)CH), 1.14 (d, $^3J_{\text{HH}} = 6.8\text{ Hz}$, 24H, CH(CH₃)₂), 1.05 (d, $^3J_{\text{HH}} = 6.8\text{ Hz}$, 12H, CH(CH₃)₂), 1.02, 0.98 (d, $^3J_{\text{HH}} = 6.8\text{ Hz}$, 6H, CH(CH₃)₂) ppm. $^{13}\text{C}\{^1\text{H}\}$ NMR (126 MHz, benzene- d_6) δ 165.4, 165.4, 165.3 (NC(CH₃)CH), 144.5, 143.9, 143.5 (*C*_{ipso}), 141.9, 141.9, 141.7 (*C*_{ortho}), 125.0, 125.0, 124.8 (*C*_{para}), 124.5, 124.3, 123.6 (*C*_{meta}), 94.6, 94.4, 94.3 (NC(CH₃)CH), 28.4, 28.3, 28.3 (CH(CH₃)₂), 25.0, 24.7, 24.6, 24.2, 24.2, 24.2 (CH(CH₃)₂), 23.6, 23.6, 23.5 (NC(CH₃)CH) ppm. ^{19}F NMR (470 MHz, benzene- d_6) δ -42.0 ppm ($^2J_{\text{HF}} = 37.3\text{ Hz}$). Repeated attempts at elemental analysis failed to provide meaningful results.

Synthesis of [(BDI)CaOPh]₂ (**8**)

Anisole (7.14 μL , 0.065 mmol) was added to a C_6D_6 solution of **1** (30 mg, 0.065 mmol) and heated at 60 $^\circ\text{C}$ overnight (*ca.* 16 hours) affording a pale-yellow solution. The resulting solution was evaporated to dryness, redissolved in hot toluene (*ca.* 0.5 ml) and cooled to room temperature to yield colourless blocks of **8** (15 mg, 42%) suitable for single crystal X-ray analysis. ^1H NMR (500 MHz, benzene- d_6) δ 7.13 - 7.06 (m, 8H, Ar-*H*), 6.66 (t, $^3J_{\text{HH}} = 7.4$ Hz, 1H, OPh-*H*_{para}), 6.38 (dm, $^3J_{\text{HH}} = 7.6$ Hz, 2H, OPh-*H*_{ortho}), 4.91 (s, 1H, NC(CH₃)CH), 3.16 (hept, $^3J_{\text{HH}} = 6.9$ Hz, 4H, CH(CH₃)₂), 1.65 (s, 6H, NC(CH₃)CH), 1.11 (d, $^3J_{\text{HH}} = 6.9$ Hz, 12H, CH(CH₃)₂), 0.81 (d, $^3J_{\text{HH}} = 6.9$ Hz, 12H, CH(CH₃)₂) ppm. $^{13}\text{C}\{^1\text{H}\}$ NMR (126 MHz, benzene- d_6) δ 166.8 (NC(CH₃)CH), 162.5 (OPh-*C*_{ipso}), 145.8 (*C*_{ipso}), 142.0 (*C*_{ortho}), 130.3 (OPh-*C*_{meta}), 124.9 (*C*_{para}), 124.3 (*C*_{meta}), 118.0 (OPh-*C*_{para}), 117.9 (OPh-*C*_{ortho}), 94.4 (NC(CH₃)CH), 28.7 (CH(CH₃)₂), 24.5 (NC(CH₃)CH), 24.3 (CH(CH₃)₂) ppm. Repeated attempts at elemental analysis failed to provide meaningful results.

Declaration of competing interest

The authors declare that they have no known competing financial interests or personal relationships that could have appeared to influence the work reported in this paper.

Acknowledgements

We thank the EPSRC (UK) for the provision of a DTP studentship (ASSW) and the University of Bath. LM is a senior member of the Institut Universitaire de France. CalMip is acknowledged for a generous grant of computing time

References

1. Smyth, M. B. *Chapter 11 in March's Advanced Organic Chemistry: Reactions, Mechanisms and Structure, 7th ed., pp. 569-641*; Wiley: Hoboken, 2013.
2. Bunnett, J. F.; Zahler, R. E. *Chem. Rev.* **1951**, *49*, 140.
3. Terrier, F. *Modern Nucleophilic Aromatic Substitution* **2013**, 1-472.
4. Rohrbach, S.; Smith, A. J.; Pang, J. H.; Poole, D. L.; Tuttle, T.; Chiba, S.; Murphy, J. A. *Angew. Chem. Int. Ed.* **2019**, *58*, 16368-16388.
5. Kwan, E. E.; Zeng, Y.; Besser, H. A.; Jacobsen, E. N. *Nature Chem.* **2018**, *10*, 917-923.
6. Ong, D. Y.; Tejo, C.; Xu, K.; Hirao, H.; Chiba, S. *Angew. Chem. Int. Ed.* **2017**, *56*, 1840-1844.
7. Ong, D. Y.; Pang, J. H.; Chiba, S. *J. Synth. Org. Chem. Jap.* **2019**, *77*, 1060-1069.
8. Barham, J. P.; Dalton, S. E.; Allison, M.; Nocera, G.; Young, A.; John, M. P.; McGuire, T.; Campos, S.; Tuttle, T.; Murphy, J. A. *J. Am. Chem. Soc.* **2018**, *140*, 11510-11518.
9. Handel, H.; Pasquini, M. A.; Pierre, J. L. *Tetrahedron* **1980**, *36*, 3205-3208.

10. Booiij, M.; Deelman, B. J.; Duchateau, R.; Postma, D. S.; Meetsma, A.; Teuben, J. H. *Organometallics* **1993**, *12*, 3531-3540.
11. Ruspic, C.; Nembenna, S.; Hofmeister, A.; Magull, J.; Harder, S.; Roesky, H. W. *J. Am. Chem. Soc.* **2006**, *128*, 15000-15004.
12. Spielmann, J.; Harder, S. *Chem. Eur. J.* **2007**, *13*, 8928-8938.
13. Harder, S. *Chem. Commun.* **2012**, *48*, 11165-11177.
14. Causero, A.; Ballmann, G.; Pahl, J.; Zijlstra, H.; Farber, C.; Harder, S. *Organometallics* **2016**, *35*, 3350-3360.
15. Causero, A.; Ballmann, G.; Pahl, J.; Farber, C.; Intemann, J.; Harder, S. *Dalton Trans.* **2017**, *46*, 1822-1831.
16. Causero, A.; Elsen, H.; Ballmann, G.; Escalona, A.; Harder, S. *Chem. Commun.* **2017**, *53*, 10386-10389.
17. Maitland, B.; Wiesinger, M.; Langer, J.; Ballmann, G.; Pahl, J.; Elsen, H.; Farber, C.; Harder, S. *Angew. Chem. Int. Ed.* **2017**, *56*, 11880-11884.
18. Rosch, B.; Gentner, T. X.; Elsen, H.; Fischer, C. A.; Langer, J.; Wiesinger, M.; Harder, S. *Angew. Chem. Int. Ed.* **2019**, *58*, 5396-5401.
19. Martin, J.; Knupfer, C.; Eyselien, J.; Farber, C.; Grams, S.; Langer, J.; Thum, K.; Wiesinger, M.; Harder, S. *Angew. Chem. Int. Ed.* **2020**, *59*, 9102-9112.
20. Martin, J.; Eyselien, J.; Grams, S.; Harder, S. *ACS Catalysis* **2020**, *10*, 7792-7799.
21. Jochmann, P.; Davin, J. P.; Spaniol, T. P.; Maron, L.; Okuda, J. *Angew. Chem. Int. Ed.* **2012**, *51*, 4452-4455.
22. Leich, V.; Spaniol, T. P.; Okuda, J. *Inorg. Chem.* **2015**, *54*, 4927-4933.
23. Leich, V.; Spaniol, T. P.; Maron, L.; Okuda, J. *Angew. Chem. Int. Ed.* **2016**, *55*, 4794-4797.
24. Schuhknecht, D.; Lhotzky, C.; Spaniol, T. P.; Maron, L.; Okuda, J. *Angew. Chem. Int. Ed.* **2017**, *56*, 12367-12371.
25. Mukherjee, D.; Schuhknecht, D.; Okuda, J. *Angew. Chem. Int. Ed.* **2018**, *57*, 9590-9602.
26. Shi, X. H.; Hou, C. P.; Zhou, C. L.; Song, Y. Y.; Cheng, J. H. *Angew. Chem. Int. Ed.* **2017**, *56*, 16650-16653.
27. Shi, X. H.; Qin, G. R.; Wang, Y.; Zhao, L. X.; Liu, Z. Z.; Cheng, J. *Angew. Chem. Int. Ed.* **2019**, *58*, 4356-4360.
28. Shi, X. H.; Hou, C. P.; Zhao, L. X.; Deng, P.; Cheng, J. H. *Chem. Commun.* **2020**, *56*, 5162-5165.
29. Martin, J.; Eyselien, J.; Langer, J.; Elsen, H.; Harder, S. *Chem. Commun.* **2020**, Advance Article.
30. Wilson, A. S. S.; Hill, M. S.; Mahon, M. F.; Dinoi, C.; Maron, L. *Science* **2017**, *358*, 1168-1171.

31. Wilson, A. S. S.; Dinoi, C.; Hill, M. S.; Mahon, M. F.; Maron, L. *Angew. Chem. Int. Ed.* **2018**, *57*, 15500-15504.
32. Dyllal, J.; Hill, M. S.; Mahon, M. F.; Teh, L.; Wilson, A. S. S. *Dalton Trans.* **2019**, *48*, 4248-4254.
33. Hill, M. S.; Mahon, M. F.; Wilson, A. S. S.; Dinoi, C.; Maron, L.; Richards, E. *Chem. Commun.* **2019**, *55*, 5732-5735.
34. Wilson, A. S. S.; Dinoi, C.; Hill, M. S.; Mahon, M. F.; Maron, L.; Richards, E. *Angew. Chem. Int. Ed.* **2020**, *59*, 1232-1237.
35. Morris, L. J.; Hill, M. S.; Manners, I.; McMullin, C. L.; Mahon, M. F.; Rajabi, N. A. *Chem. Commun.* **2019**, *55*, 12964-12967.
36. Bauer, H.; Thum, K.; Alonso, M.; Fischer, C.; Harder, S. *Angew. Chem. Int. Ed.* **2019**, *58*, 4248-4253.
37. Brand, S.; Elsen, H.; Langer, J.; Grams, S.; Harder, S. *Angew. Chem. Int. Ed.* **2019**, *58*, 15496-15503.
38. Wilson, A. S. S.; Hill, M. S.; Mahon, M. F. *Organometallics* **2019**, *38*, 351-360.
39. Zhao, X. F.; Xiao, D. M. F.; Cui, X. L.; Chai, C. Q.; Zhao, L. L. *Catal. Sci. & Tech.* **2020**, *10*, 950-958.
40. Harder, S. *Organometallics* **2002**, *21*, 3782-3787.
41. Bonyhady, S. J.; Jones, C.; Nembenna, S.; Stasch, A.; Edwards, A. J.; McIntyre, G. J. *Chem. Eur. J.* **2010**, *16*, 938-955.
42. Shannon, R. D. *Acta Cryst. A* **1976**, *32*, 751-767.
43. Ruspic, C.; Harder, S. *Inorg. Chem.* **2007**, *46*, 10426-10433.
44. Beak, P.; Brown, R. A. *J. Org. Chem.* **1977**, *42*, 1823-1824.
45. Mortier, J.; Moyroud, J.; Bennetau, B.; Cain, P. A. *J. Org. Chem.* **1994**, *59*, 4042-4044.
46. Whisler, M. C.; MacNeil, S.; Snieckus, V.; Beak, P. *Angew. Chem. Int. Ed.* **2004**, *43*, 2206-2225.
47. Macklin, T. K.; Snieckus, V. *Org. Lett.* **2005**, *7*, 2519-2522.
48. Roberts, J. D.; Curtin, D. Y. *J. Am. Chem. Soc.* **1946**, *68*, 1658-1660.
49. Schlosser, M.; Katsoulos, G.; Takagishi, S. *Synlett* **1990**, *1990*, 747-748.
50. Garden, J. A.; Armstrong, D. R.; Clegg, W.; García-Alvarez, J.; Hevia, E.; Kennedy, A. R.; Mulvey, R. E.; Robertson, S. D.; Russo, L. *Organometallics* **2013**, *32*, 5481-5490.
51. Armstrong, D. R.; Blair, V. L.; Clegg, W.; Dale, S. H.; Garcia-Alvarez, J.; Honeyman, G. W.; Hevia, E.; Mulvey, R. E.; Russo, L. *J. Am. Chem. Soc.* **2010**, *132*, 9480-9487.
52. Uchiyama, M.; Naka, H.; Matsumoto, Y.; Ohwada, T. *J. Am. Chem. Soc.* **2004**, *126*, 10526-10527.
53. Baillie, S. E.; Bluemke, T. D.; Clegg, W.; Kennedy, A. R.; Klett, J.; Russo, L.; de Tullio, M.; Hevia, E. *Chem. Commun.* **2014**, *50*, 12859-12862.

54. Martínez-Martínez, A. J.; Kennedy, A. R.; Mulvey, R. E.; O'Hara, C. T. *Science* **2014**, *346*, 834-837.
55. Whisler, M. C.; MacNeil, S.; Snieckus, V.; Beak, P. *Angewandte Chemie International Edition* **2004**, *43*, 2206-2225.
56. Gilman, H.; Bebb, R. L. *J. Am. Chem. Soc.* **1939**, *61*, 109-112.
57. Wittig, G.; Fuhrmann, G. *Ber. Dtsch. Chem. Ges. B* **1940**, *73*, 1197-1218.
58. Bauer, W.; Schleyer, P. v. R. *J. Am. Chem. Soc.* **1989**, *111*, 7191-7198.
59. Saa, J. M.; Deya, P. M.; Suner, G. A.; Frontera, A. *J. Am. Chem. Soc.* **1992**, *114*, 9093-9100.
60. Stratakis, M. *J. Org. Chem.* **1997**, *62*, 3024-3025.
61. Harder, S.; Boersma, J.; Brandsma, L.; van Mier, G. P. M.; Kanters, J. A. *J. Organometal. Chem.* **1989**, *364*, 1-15.
62. Clegg, W.; Dale, S. H.; Drummond, A. M.; Hevia, E.; Honeyman, G. W.; Mulvey, R. E. *J. Am. Chem. Soc.* **2006**, *128*, 7434-7435.
63. Mulvey, R. E.; Armstrong, D. R.; Conway, B.; Crosbie, E.; Kennedy, A. R.; Robertson, S. D. *Inorg. Chem.* **2011**, *50*, 12241-12251.
64. Clegg, W.; Conway, B.; García-Álvarez, P.; Kennedy Alan, R.; Mulvey Robert, E.; Russo, L.; Sassmannshausen, J.; Tuttle, T. *Chem. Eur. J.* **2009**, *15*, 10702-10706.
65. Weigert, F. J. *J. Org. Chem.* **1980**, *45*, 3476-3483.
66. Nembenna, S.; Roesky, H. W.; Nagendran, S.; Hofmeister, A.; Magull, J.; Wilbrandt, P. J.; Hahn, M. *Angew. Chem. Int. Ed.* **2007**, *46*, 2512-2514.
67. Barrett, A. G. M.; Crimmin, M. R.; Hill, M. S.; Hitchcock, P. B.; Procopiou, P. A. *Angew. Chem. Int. Ed.* **2007**, *46*, 6339-6342.
68. Fulmer, G. R.; Miller, A. J. M.; Sherden, N. H.; Gottlieb, H. E.; Nudelman, A.; Stoltz, B. M.; Bercaw, J. E.; Goldberg, K. I. *Organometallics* **2010**, *29*, 2176-2179.
69. Deacon, G. B.; Forsyth, C. M.; Junk, P. C. *J. Organometal. Chem.* **2000**, *607*, 112-119.
70. Boyle, T. J.; Hernandez-Sanchez, B. A.; Baros, C. M.; Brewer, L. N.; Rodriguez, M. A. *Chem. Mater.* **2007**, *19*, 2016-2026.
71. Deacon, G. B.; Junk, P. C.; Moxey, G. J.; Ruhlandt-Senge, K.; St. Prix, C.; Zuniga, M. F. *Chem. Eur. J.* **2009**, *15*, 5503-5519.
72. Deacon, G. B.; Junk, P. C.; Moxey, G. J.; Guino-o, M.; Ruhlandt-Senge, K. *Dalton Trans.* **2009**, 4878-4887.
73. Pratt, D. A.; de Heer, M. I.; Mulder, P.; Ingold, K. U. *J. Am. Chem. Soc.* **2001**, *123*, 5518-5526.
74. Luo, Y. R. *Comprehensive Handbook of Chemical Bond Energies*; CRC Press: Boca Raton, FL, 2007.
75. Maercker, A. *Angew. Chem. Int. Ed. Engl.* **1987**, *26*, 972-989.

76. Causero, A.; Ballmann, G.; Pahl, J.; Farber, C.; Intemann, J.; Harder, S. *Dalton Trans.* **2017**, 46, 1822-1831.
77. Werkema, E. L.; Yahia, A.; Maron, L.; Eisenstein, O.; Andersen, R. A. *New J. Chem.* **2010**, 34, 2189-2196.

For Table of Contents:

